

Study on Corrosion Performance of Cu-Te-Se Alloys in a 3.5% Sodium Chloride Solution

Lin Jiao, Meng Li, Tao Zeng, and Dachuan Zhu

(Submitted December 2, 2014; in revised form August 31, 2015; published online October 22, 2015)

Samples of Cu-Te-Se alloys, previously aged or treated as a solid solution, were immersed in 3.5% (mass fraction) sodium chloride solution to investigate their corrosion resistance at room temperature by determining their corrosive weight loss. The morphologies of the precipitated phase and surface products following immersion were observed by scanning electron microscope. In addition, energy-dispersive spectroscopic analysis was used to determine the elemental constituents of precipitated phase and corroded surface of the alloy samples. The phase composition was measured by x-ray diffraction, and the electrochemical polarization behavior of the samples was determined using an electrochemical workstation. The experimental results revealed that the alloy samples appeared to corrode uniformly, which was accompanied by a small amount of localized corrosion. There was the possibility that localized corrosion could increase following aging treatment. The addition of a small amount of tellurium and selenium to the alloy appeared to retard oxygen adsorption on the copper in the alloy, which has ameliorated the alloy corrosion due to the similar physical and chemical properties of oxygen. In comparison to the solid solution state, the corrosion resistance of the alloy appeared to decline slightly following aging treatment.

Keywords aging treatment, Cu-Te-Se alloys, electrochemical corrosion, immersion corrosion, solid solution treatment

1. Introduction

Copper and copper alloys are widely used in electrical engineering, light industry, machinery manufacturing, building industry, national defense industry, and many other fields, due to their excellent electrical conductivity, thermal conductivity, corrosion resistance, and processing performance (Ref 1-5). The high strength of pure copper resulting from cold-rolled deformation is easily lost in the process of annealing (Ref 6-8). Consequently, it is highly desirable to study the high strength and high conductivity copper alloys. Previous researchers have shown that, by adopting different processing technologies, the tensile strength of copper alloys can be improved by addition of tellurium to pure copper, which can increase the tensile strength of the resulting alloy to 500 MPa while maintaining the alloy's electrical conductivity at 94~98% of the International Annealing Copper Standard (IACS) (Ref 9). Although the Cu-Te alloy has excellent electrical and mechanical properties, this application is limited, because tellurium is a rare commodity and is considered a strategic resource. In addition, the market price of tellurium is much higher than selenium. Since selenium is in the same group as tellurium in the Periodic Table, the two have similar physical and chemical properties. Considering the scarcity and cost of tellurium, in this study, selenium was

chosen to replace some of the tellurium in the copper alloys in an attempt to develop Cu-Te-Se alloys with properties similar to the Cu-Te alloy.

Achieving high strength and high conductivity in the alloy is the first step after which more work will be needed to further refine the properties of these alloys. Extended exposure to oxygen or moist environments will cause copper to corrode which compromises the properties of the product. The existence of the salt in these environments can significantly increase corrosion rate of the pure metal or copper alloy (Ref 10-14). Even solid salt will also accelerate the corrosion of copper metal (Ref 13, 15). Research in developed countries has been intensive in the study of corrosion of copper and copper alloys (Ref 16-19).

To broaden the commercial application of Cu-Te-Se alloys, the corrosion resistance of Cu-Te-Se alloys in 3.5% sodium chloride solution was chosen as the focus of the study reported here. A review of the current literature failed to reveal any related research reports concerning the corrosion of Cu-Te-Se alloy in salt solution. Therefore, based on the practical engineering applications, industrially pure copper and copper alloys with various tellurium and selenium contents were subjected to select heat treatment and then immersed in 3.5% sodium chloride solution to determine their corrosion resistance at room temperature. In addition, the corrosion mechanism of the alloys is discussed to stimulate efforts to develop new alloys that can be introduced into practical production.

2. Materials and Methods

The copper alloy ingots were smelted in ZG-25 Vacuum Induction Furnace by adding different amounts of tellurium and selenium into industrial pure copper. The contents of tellurium and selenium in the ingots were determined by ADVAN-XRF, and the results of the analysis are shown in Table 1. The ingots

Jiao Lin, Zeng Tao, and Zhu Dachuan, School of Materials Science and Engineering, Sichuan University, P.O. Box 610065, Chengdu, China; and Li Meng, School of Aeronautical Engineering, Civil Aviation Flight University of China, P.O. Box 618307, Guanghan, China. Contact e-mail: zhudachuan@scu.edu.cn.

Table 1 The designed and measured content of Te and Se

No. of samples	1#	2#	3#
Designed content of Se	...	0.15	0.25
Designed content of Te	...	0.15	0.25
Measured content of Se	...	0.109	0.149
Measured content of Te	...	0.125	0.243

were heated to 850 °C, held for 4 h, and then forged into copper plates with a thickness of 18 mm.

The hot-forged copper alloys were cut into cubic samples with dimensions of 10 × 10 × 10 mm using a wire electrode. The samples were reheated to 850 °C and maintained at this temperature for 2 h, and then, the samples were quenched in water to room temperature. After this, the samples were divided into two groups: One group was processed no further, while the other group was reheated to 420 °C and maintained at this temperature for 4 h as an aging treatment and cooled in the furnace to room temperature. The samples were burnished with 800 grit sand paper and then polished. All the samples were washed with acetone and doubly distilled water and then dried. The length of each side was measured using a Vernier caliper, and the total surface area was calculated. Then, each sample was suspended and immersed in 3.5% sodium chloride solution. The samples were removed from solution every 120 h, and the corrosion products were washed off with a moderate amount of alcohol in a KH2200DB numerical controlled ultrasonic cleaner. Following this procedure, the samples were dried using an electric hair drier. The mass of the samples was measured using a model FA1204 electronic precision balance with an accuracy of 0.1 mg. Finally, the weight loss per unit area of each sample was calculated. The corrosion products on the surface of samples were analyzed, and the phase composition was determined using a X'Pert Pro MPD type XRD manufactured by the Philips Company. A JSM-5910LV type scanning electron microscope (SEM) was used to inspect the morphology of the corrosion products on the surface, and energy-dispersive spectroscopy (EDS) was used to measure the composition of corrosion products and the precipitated phases. The electrochemical polarization behavior of each sample in 3.5% sodium chloride solution was determined using an electrochemical workstation. Based on these results, the main corrosion process and corrosion mechanism were determined.

3. Results

3.1 Microstructure and Precipitated Phase Analysis

The microstructure of the alloys is shown in Fig. 1. In Sample #3, very little of the second phase was evident following the after solid solution treatment, but there was significant amount of the precipitated phase present in the alloys following the aging treatment. The quantity of precipitated phase of Sample #3 appeared to be greater than that in Sample #2, because of the different selenium and tellurium contents of these two alloys as is evident as shown in Fig. 1(a) and (c). The elemental composition of the precipitated phase marked as plots A and B in these figures was determined by

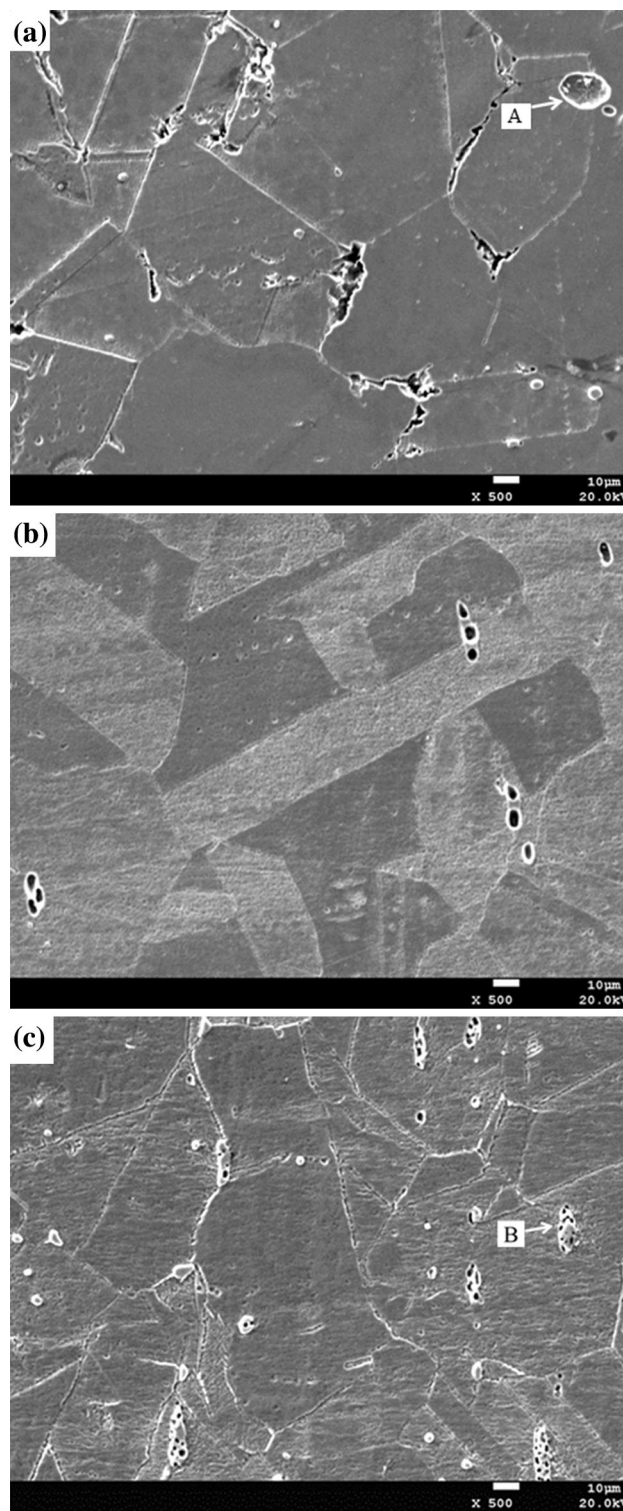


Fig. 1 The microstructure and distribution of precipitated phase of samples. (a) aging of 2#; (b) solid solution of 3#; (c) aging of 3#

EDS, and the results are shown in Fig. 2 and Table 2. The precipitated phase x-ray diffraction (XRD) spectrum is shown in Fig. 3, where it can be seen that only copper was found. This result may be due to the small quantity of the precipitated phase which is not sufficient for XRD analysis. According to the mass ratio and atomic ratio of the precipitated phase as shown in

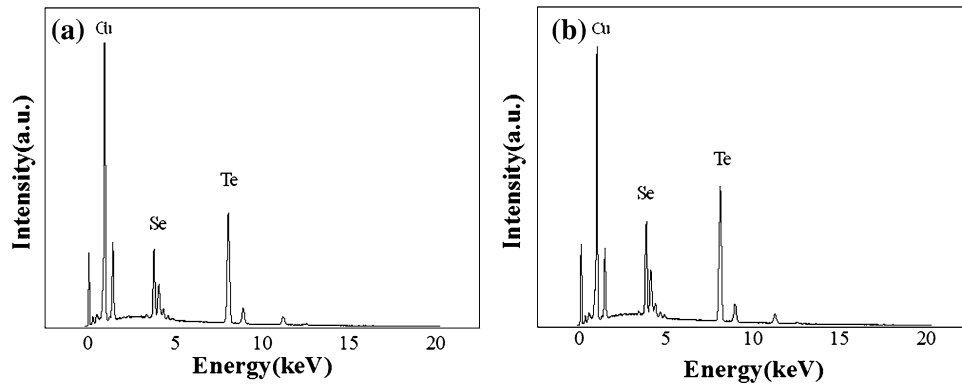


Fig. 2 The EDS spectrum of precipitated phase of alloys

Table 2 The EDS test results of precipitated phase

Elements	A		B	
	ω, %	at.%	ω, %	at.%
Cu K	56.27	67.40	58.31	69.32
Se L	17.74	17.10	16.44	15.73
Te L	26.00	15.51	25.25	14.95
Total	100.00			

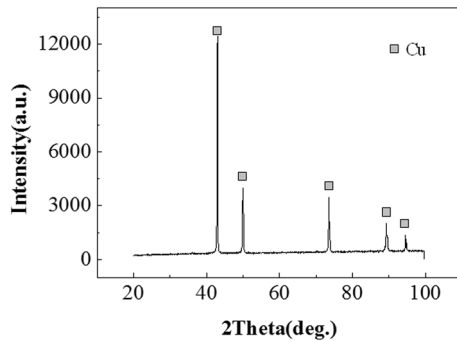


Fig. 3 The XRD spectrum of precipitated phase analysis

Table 2, it can be concluded that the precipitated phase was probably composed of Cu_2 (Te, Se).

3.2 Polarization Curves

The polarization curves for the alloys in 3.5% sodium chloride solution following the two heat treatments are shown in Fig. 4, and the corrosion potential and corrosion current density of the alloys are listed in Table 3. As summarized in Table 3, it can be seen that the corrosion current density of the aging treatment samples was greater than the current density of the solid solution treatment samples, indicating that the aging treatment alloys were more likely to corrode.

3.3 Weight Loss Measurements

Based on the results of passive sample corrosion tests and the sample weight loss in the corrosion process, the corrosion rate was calculated using the national standard GB10124-88, the equation for this is as follows:

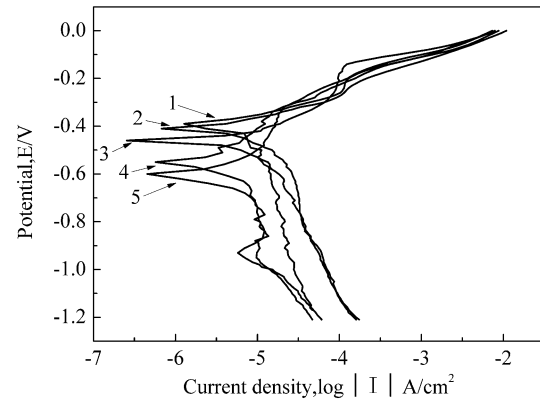


Fig. 4 Polarization curves of samples in 3.5% sodium chloride solution. 1—Aging of 2#; 2—solid solution of 2#; 3—pure copper; 4—solid solution of 3#; 5—aging of 3#

$$R = 8.76 \times 10^7 \times (M - M_t) / STD. \quad (\text{Eq 1})$$

Here, R (mm/a) is the corrosion rate; M (g) is the mass of the samples before test; M_t (g) is the mass of the samples after a period of experimental time T ; S (cm^2) is the area of the sample; T (h) is the test time; and D (kg/m^3) is the density of material.

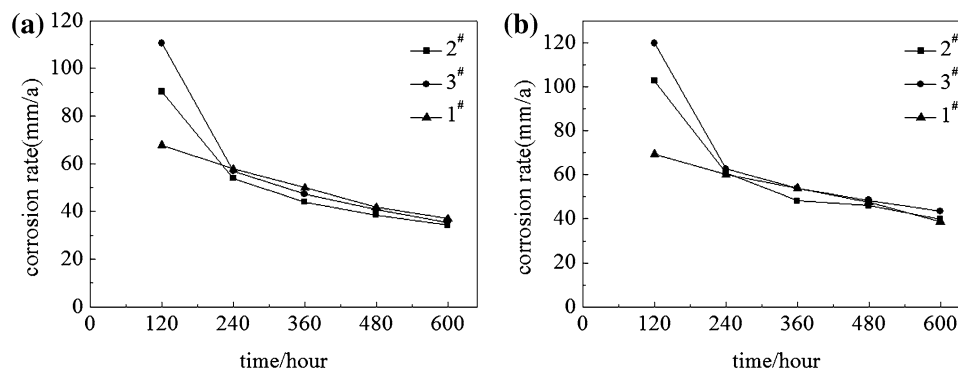
As shown in Fig. 5, at the beginning of the experiment, there was a large difference among the corrosion rates of Samples #1-3 based on the heat treatment employed, but this difference gradually decreased with time. The corrosion rates equalized after about 240 h of immersion. Generally speaking, the corrosion rate of the alloys following aging treated was slightly higher than that of the alloys subjected to the solid solution treatment.

3.4 Morphology of Corrosion Surface Analysis

Fig. 6 shows the SEM analysis of the morphologies of alloys' corrosion surface after corroding for 600 h. It can be seen that the Sample #2 exhibited a similar degree of corrosion as Sample #3 degree when both were solid solution treated. However, Sample #3 exhibited more significant corrosion than Sample #2 when both were after aging treated. As can be seen from Fig. 6(b), solid solution-treated Sample #3 exhibited nearly no localized corrosion. By contrast, the corrosion morphology of aging treated Sample #3 exhibited clear grain boundary corrosion as shown in Fig. 6(d). These results

Table 3 Corrosion potential and corrosion current density of alloys

	Pure copper	Aging of 3#	Aging of 2#	Solid solution of 3#	Solid solution of 2#
E_{corr} , mV	-460.7	-600	-391.1	-549.1	-409.8
I_{corr} , $\mu\text{A}/\text{cm}^2$	7.4881	3.9171	3.7922	2.5529	2.2356

**Fig. 5** The corrosion rate of samples in 3.5% sodium chloride solution. (a) Solid solution treatment; (b) aging treatment

suggest that the corrosion of the solid solution-treated alloys was more significant than the aging treated alloys.

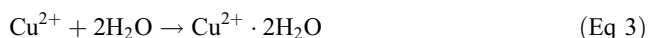
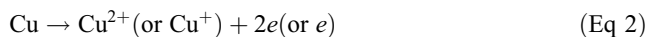
3.5 Analysis of the Corrosion Surface Phase

The results of EDS spectrum analysis of the corroded alloys surfaces are shown in Fig. 7 and Table 4. The phase analysis results of surface corrosion of the samples are shown in Fig. 8. According to Fig. 8, the main corrosion products appeared to copper and cuprous oxide, but the EDS test results showed that the elemental constituents of corrosion product were not just copper and oxygen, but chlorine was also present. Considering the content of the corrosion bath, this is hardly surprising. Comparing the EDS with XRD test results, the corrosion products of various samples were generally identical, as would be expected.

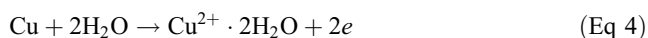
4. Analysis and Discussion

When immersed in 3.5% sodium chloride solution at room temperature, a very thin water film containing chloride ions formed on the sample surface, thus the manner of sample corrosion was electrochemical corrosion (Ref 20). According to the experimental results shown above, the corresponding corrosion reaction processes could be inferred as follows:

The anode reaction: metal dissolved in the solution in the form of hydrated ion and electrons remained at the metal surface. Simultaneously, electrons from the anode flowed to the cathode:



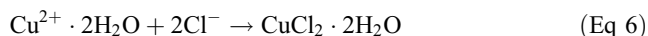
or



The cathode reaction: oxygen adsorbed on the cathode surface by diffusion or convection, and then absorbed the surplus electrons on metal surface to form hydroxyl ions, namely:



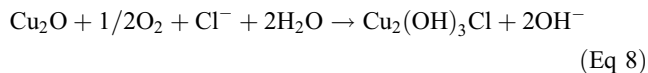
With the dissolution of sodium chloride, the corrosion products were formed by the reaction of chloride ion and hydration of copper ion (or copper ion) (anodic reaction products), namely:



or



In addition, the corrosive liquid and samples were kept at a stationary state during the experimental process, thus cuprous ions would accumulate on the surface of the sample leading to a local supersaturated solution on the sample surface. Cuprous oxide (Fig. 8) formed when cuprous ions reacted with oxygen in solution. After its formation, cuprous oxide would expand into the surrounding surface by continuous accumulation of cuprous ions, thus a degree of cuprous oxide crystal film was formed on the sample surface. Simultaneously, due to the presence of reducing chlorine ions in the solution, part of the cuprous oxide was converted into alkaline copper chloride, which remained on the surface of the cuprous oxide, under the action of chloride ions and oxygen in the solution (Ref 21), namely:



Since the quantity of alkaline copper chloride was small and the corrosion products were removed during experimental ultrasonic cleaning process, the alkaline copper chloride could not be detected by the XRD (Fig. 8). However, the EDS results for the corrosion products confirmed that chlorine was present in the products (Fig. 7).

The corrosion rate of the samples (Fig. 5) was relatively rapid at the beginning of the experiment, but it gradually slowed as the experiment proceeded. This occurred because a patina was formed on the surface of the copper alloy during the

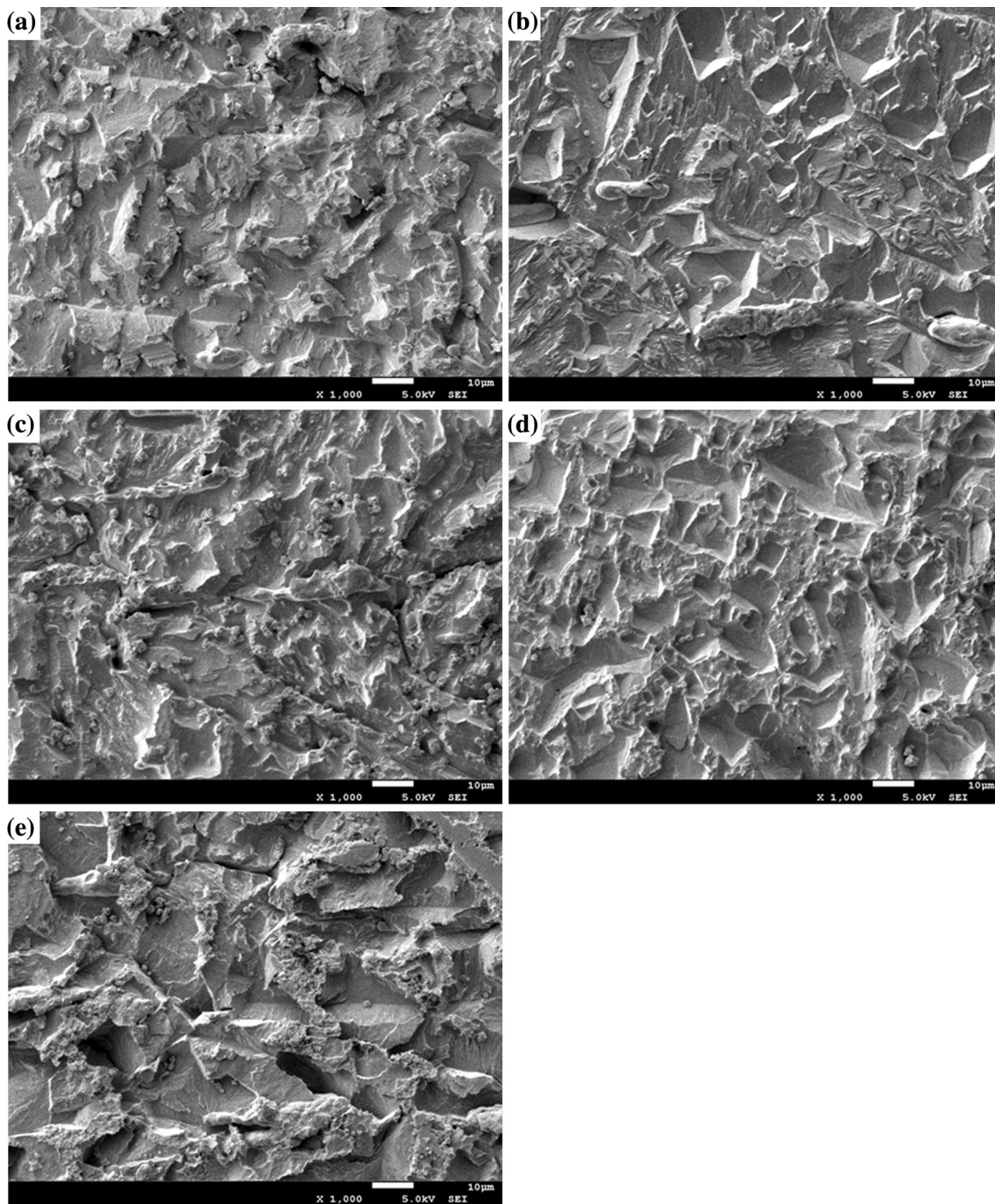


Fig. 6 The morphology of corrosion surface of samples. (a) Solid solution of Sample 2#; (b) solid solution of Sample 3#; (c) aging of Sample 2#; (d) aging of Sample 3#; (e) pure copper

corrosion process, which slowed the rate of corrosion (Ref 22-24). Concurrently, since the samples were completely exposed early in the experiment, the diffusion and convection of oxygen to the metal surface was facilitated. Therefore, the samples' corrosion rate was rapid at the outset of the experiment. As the time of immersion proceeded, the cumulative amount of corrosion products gradually increased on the samples surface and the corrosion rate decreased by this accumulation of corrosion products until it became constant. Since the chloride ion has a small radius with strong penetrating power, it can easily cross the surface of metal corrosion product layer and

cause corrosion in the internal part of the metal. The metal chlorides formed gradually and dissolved easily, so that the corrosion process achieved a dynamic balance, and the rate of corrosion rate eventually becomes static. This is similar to the corrosion behavior of copper and copper alloy in the atmosphere. However, the time required for the development of a constant corrosion rate depends on the experimental environment (Ref 25-27).

The solid solution treatment alloy samples exhibited polarization curves that showed a higher polarization potential (Fig. 4) and smaller corrosion current density (Table 3).

Therefore, it can be concluded that these samples had better corrosion resistance (Fig. 5). A quantity of a precipitated phase appeared on the grain boundary of the aging treated samples (Fig. 1a and c), which can be estimated to be $\text{Cu}_2(\text{Te}, \text{Se})$ (Table 2). The standard electrode potentials of the precipitated phase $\text{Cu}_2(\text{Te}, \text{Se})$ and copper matrix were different. Therefore, the precipitated phase and copper matrix formed a microcell

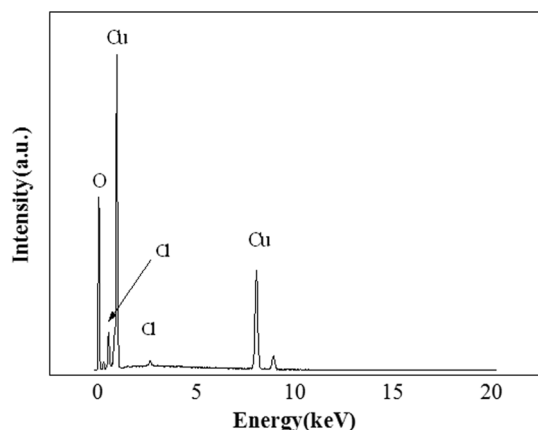


Fig. 7 The EDS spectrum of sample corrosion surface products

Table 4 The EDS test results of corrosion surface

Elements	$\omega, \%$	at. %
O K	14.79	40.60
Cl K	0.94	1.17
Cu K	84.26	58.23
Total	100.00	

during the corrosion process, which resulted in a faster corrosion rate (Fig. 5). But when a small amount of tellurium and selenium was added to industrially pure copper, the non-metallic impurity in the copper was reduced, thereby eliminating corrosion along the grain boundary (Ref 28). Based on these two effects, the corrosion properties of the alloy containing tellurium and selenium with different heat treatments appear to behave differently. The polarization curves (Fig. 4) also showed that the electrode potential decreased and corrosion current density increased after the aging treatment. In addition, as shown in the corrosion surface morphology (Fig. 6b and d), the corrosion of Sample #3 was more extensive after the aging treatment than after the solid solution treatment. This confirms the effect of aging on the corrosion resistance of alloys. For the same composition samples, the corrosion resistance was slightly lower after aging than that of solid solution state.

Based on the microstructure of the alloys (Fig. 1a and c), Sample #3 had more of the precipitated phase at the grain boundary and intracrystalline material than Sample #2 following aging treatment. This increased the lability of Sample #3 to corrosion over that of Sample #2. The morphology of corrosion surface of alloys (Fig. 6), the polarization curves (Fig. 4) and corrosion rate (Fig. 5b) suggest that the corrosion resistance of Sample #2 was better than that of Sample #3#. Comparing Samples of #2 and #3 with pure copper (Sample #1) at the beginning of the experiment, (because the precipitated phase existed in microstructures of 2# and 3# Samples) the precipitated phase and copper matrix would form a microcell during the corrosion process, which would result in a faster corrosion rate for Samples #2 and #3 than Sample #1. However, selenium and tellurium are in the same group with oxygen in the Periodic Table, so they may have similar physical and chemical properties. While the main corrosion mechanism of copper is oxygen adsorption corrosion, this process may be retarded as

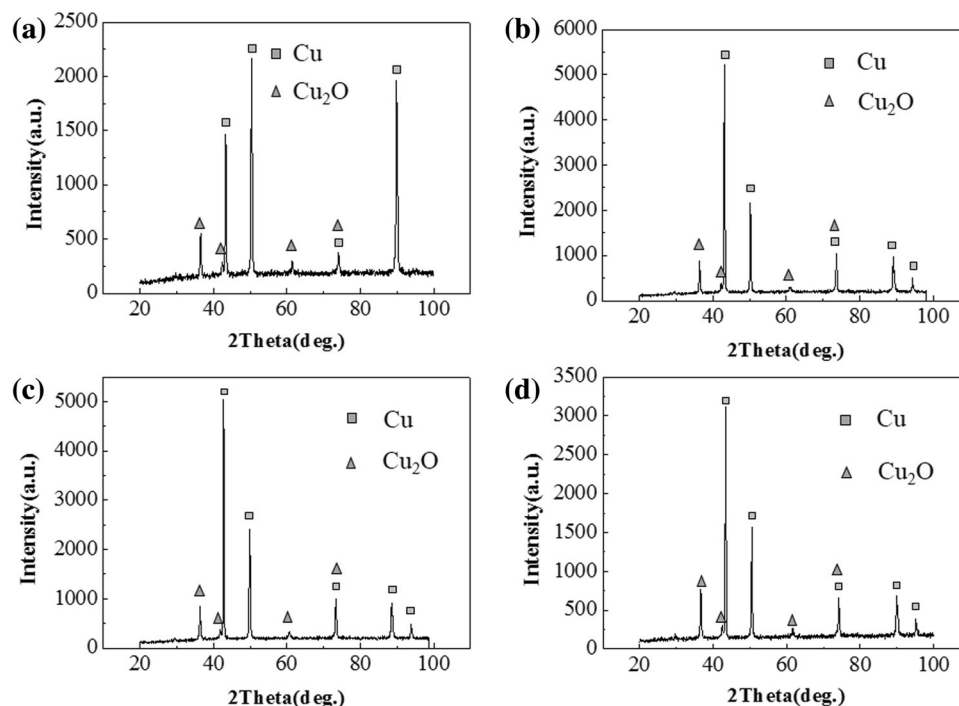


Fig. 8 The XRD spectrum of samples corrosion surface products phase analysis. (a) Pure copper; (b) aging of 2#; (c) solid solution of 3#; (d) aging of 3#

the experiment proceeds by the presence of selenium and tellurium in the alloy. As a result, the corrosion rate of Samples #2 and #3 gradually equaled or was less than that of Sample #1.

5. Conclusions

- (i) When immersed in 3.5% sodium chloride solution, corrosion of Cu-Te-Se alloys at room temperature was uniform, accompanied by a small amount of localized corrosion. The localized corrosion trended to increase after the samples were aging treated. The main corrosion mechanism of the samples was electrochemical corrosion.
- (ii) The addition of tellurium and selenium to industrially pure copper produced a precipitate on the surface which passivated the surface, slowing the corrosion rate. It appeared that adding a small amount of tellurium and selenium to copper slowed the process of oxygen adsorption on the copper due to the similar physical and chemical properties of these elements to oxygen.
- (iii) Following the aging treatment, the Cu-Te-Se alloys developed a second phase precipitate, and the polarization current density of precipitated phase was different than that of the copper matrix. As a result, the corrosion resistance of Cu-Te-Se alloys after aging was decreased compared with the alloys after solid solution treatment.

Acknowledgment

The authors thank the Project (2012BAE06B01-04) supported by the National Science & Technology Pillar Program of China.

References

1. S.H. Hong, H.T. Jeong et al., Deformation and Recrystallization Textures of Surface Layer of Copper Sheet, *Mater. Sci. Eng. A.*, 1997, **229**, p 174–181
2. X.W. Li, D.T. Zhang et al., Microstructure and Mechanical Properties of Dissimilar Pure Copper/1350 Aluminum Alloy Butt Joints by Friction Stir Welding, *Trans. Nonferrous Met. Soc. China*, 2012, **22**, p 1298–1306
3. S. Raygan, H. Ehsanian Mofrad, M. Pourabduli, and F.K. Ahadi, Effect of Rolling and Annealing Processes on the Hardness and Electrical Conductivity Values of Cu-13.5%Mn-4%Ni Alloy, *J. Mater. Process. Technol.*, 2011, **211**, p 1810–1816
4. A. Kauffmann and J. Freudenberg, Severe Deformation Twinning in Pure Copper by Cryogenic Wire Drawing, *Acta Mater.*, 2011, **59**, p 7816–7823
5. M. Yang and Z.Y. Wang, Review of Atmospheric Corrosion of Copper, *Equip. Environ. Eng.*, 2006, **3**(4), p 38–44
6. T. Konkova, S. Mironov et al., Microstructural Response of Pure Copper to Cryogenic Rolling, *Acta Mater.*, 2010, **58**, p 5262–5273
7. X.T. Wang, *Metal Materials Science*, Mechanical Industry Press, Beijing, 1987
8. X.Y. Jiang and Y.L. Li, Copper Alloy of High Strength and High Conductivity, *Shanghai Nonferrous Met.*, 1995, **16**(5), p 284–288
9. D.C. Zhu, M.Z. Song, and D.M. Yang, Study on the Oxidation Resistance of Cu₂Te Alloys with High Electrical Conductivity, *Funct. Mater.*, 2004, **13**, p 713–715
10. V. Rosa, D. Diana, and M.R. Blanca, Effect of Atmospheric Pollutants on the Corrosion of High Power Electrical Conductors—Part 2. Pure Copper, *Corros. Sci.*, 2007, **49**(6), p 2329–2350
11. J. Sandberg, I.O. Wallinder, and C. Leygraf, Corrosion-Induced Copper Runoff from Naturally and Pre-patinated Copper in a Marine Environment, *Corros. Sci.*, 2006, **48**(12), p 4316–4338
12. F. Corvo, J. Minotas, and J. Delgado, Changes in Atmospheric Corrosion Rate Caused by Chloride-Ions Depending on Rain Regime, *Corros. Sci.*, 2005, **47**(4), p 883–892
13. A. Drach, I. Tsukrov, J. DeCew et al., Field Studies of Corrosion Behaviour of Copper Alloys in Natural Seawater, *Corros. Sci.*, 2013, **76**, p 453–464
14. X. Zhang, I.O. Wallinder, and C. Leygraf, Mechanistic Studies of Corrosion Product Flaking on Copper and Copper-Based Alloys in Marine Environments, *Corros. Sci.*, 2014, **85**, p 15–25
15. C.I.S. Santos, M.H. Mendonca, and I.T.E. Fonseca, Corrosion of Brass in Natural and Artificial Seawater, *J. Appl. Electrochem.*, 2006, **36**, p 1353–1359
16. M. Morcillo, E. Almeida, and M. Marrocos, Atmospheric Corrosion of Copper in Ibero-America, *Corrosion*, 2001, **57**(11), p 967–980
17. A.U. Leuenberger-Minger, B. Buchmann, and M. Faller, Dose-Response Functions for Weathering Steel, Copper and Zinc Obtained from a Four-Year Exposure Programme in Switzerland, *Corros. Sci.*, 2002, **44**(8), p 675–687
18. D. Knotkova, B. Bosek, and J. Vlickova, *Corrosion in Natural Environments*, ASTM, West Conshohocken, PA, 1974
19. L.P. Costas, *Atmospheric Corrosion of Copper Alloys Exposed for 15 to 20 Years*, ASTM, PA, 1982
20. H. Strandberg and L.G. Johansson, Some Aspects of the Atmospheric Corrosion of Copper in the Presence of Sodium Chloride, *J. Electrochem. Soc.*, 1998, **145**(4), p 1093–1100
21. M.L. Carvalho, J. Doma, M. Szttyler et al., The Study of Marine Corrosion of Copper Alloys in Chlorinated Condenser Cooling Circuits: The Role of Microbiological Components, *Bioelectrochemistry*, 2014, **97**, p 2–6
22. A. Kratschmer, I.O. Wallinder, and C. Leygraf, The Evolution of Outdoor Copper Patina, *Corros. Sci.*, 2002, **44**(3), p 425–450
23. K.P. Fitzgerald, J. Nairn, and A. Atrens, The Chemistry of Copper Patination, *Corros. Sci.*, 1998, **40**(12), p 2029–2050
24. B. Rosales, R. Vera, and G. Moriena, Evaluation of the Protective Properties of Natural and Artificial Patinas on Copper(I)—Patinas Formed by Immersion, *Corros. Sci.*, 1999, **41**(4), p 625–651
25. G. Haynes and R. Baboian, *Atmospheric Corrosion Behavior of Clad Metals, Degradation of Metals in the Atmosphere*, ASTM STP 965, Philadelphia, 1988
26. S. Feliu, M. Morrcillo, Jr., and S. Feliu, The prediction of Atmospheric Corrosion from Meteorological and Pollution Parameters(I)—Annual Corrosion, *Corros. Sci.*, 1993, **34**(3), p 403–414
27. S. Feliu, M. Morrcillo, Jr., and S. Feliu, The Prediction of Atmospheric Corrosion from Meteorological and Pollution Parameters(II)—Long-term Forecasts, *Corros. Sci.*, 1993, **34**(3), p 415–422
28. D.C. Zhu, C.K. Zhu, and Y. Sun, Study on the Corrosion Behavior of Cu-Te Alloy in Saturated NH₄Cl Solution, *Rare Metal Mater. Eng.*, 2007, **36**(03), p 143–145